**SERBIAN JOURNAL OF ELECTRICAL ENGINEERING**
**Vol. 16, No. 2, June 2019, 161-180**

**UDC: 621.313.332:519.6** **DOI: https://doi.org/10.2298/SJEE1902161S**

# Nonlinear Optimization of Proportional-Integral Controller in Doubly-Fed Induction Generator Using the Gradient Extremum Seeking Algorithm

**Aleksandar A. Sarić[1], Aleksandra Lj. Marjanović[2]**

**Abstract:** This paper deals with the problem of nonlinear optimization of proportional-integral (PI) controller in doubly-fed induction generator (DFIG), modeled by the detailed differential-algebraic equations (DAEs), and connected to a power system, where rest of the power system is represented only by measurements in connection point. The basic functions of PI controllers are secondary regulation of speed–active power and reactive power–voltage of multiple DFIGs connected in the same point (typical situation in wind farms). In the presence of PI controllers, stability of the transient responses depends largely on its parameters (proportional and integral part). To calculate optimal parameters of the PI controllers, an 'Extremum Seeking' (ES) algorithm was used, more precisely, its version that assumes that gradient can be calculated [hence the name 'Gradient Extremum Seeking' (GES)]. Optimization of the PI controller parameters is performed for a list of major disturbance trajectories recorded in historical database. The results obtained using the IEEE 14-bus test system show that PI controller parameters must be carefully chosen. Their effect on transient responses and stability of the power system with major disturbance (short circuit, outage etc.) conditions was additionally studied.

**Keywords:** Power system, Doubly-fed induction generator (DFIG), Proportional-integral (PI) regulator, Nonlinear parameter optimization, Gradient Extremum Seeking (GES).

## 1 Introduction

Dynamic models of the power system elements are basic tool used to analyze different phenomena, such as for example, electromechanical oscillations in transient responses (with list of major disturbances, like the short circuits, branch outages etc.). However, power system models grow up rapidly [in terms of number of elements and especially number of differential-algebraic equations (DAEs)], which makes them too complicated for practical use. In general, increasing the complexity of the model does not increase its accuracy,

[1]Prvog oktobra 4A/24, 32000 Čačak, Serbia; E-mail: aleksandar.saric.95@gmail.com
[2]School of Electrical Engineering, University of Belgrade, Bulevar kralja Aleksandra 73, 11000 Belgrade, Serbia; E-mail: amarjanovic@etf.bg.ac.rs

for several reasons: 1) insufficiently accurate model parameters, which can even vary in time, 2) lack of exchange of model parameters between individual entities, 3) not taking into consideration certain effects while building a model (for example, saturation) etc. All this leads to the difficulty of reconstructing large disturbances in the power systems and understanding their cause (notable example of this was 2003 major grid blackout in North America [1]). Another important fact is that power systems are widely equipped with sensors, which are used to keep track of various measurements, but this data is rarely used for real-time operation.

To properly identify stability problems and take appropriate preventive control measures, it is necessary to have accurate model parameters. However, the situation in real-world practice is completely opposite, as manufacturers generally do not provide a complete set of accurate data. To make matters worse, these parameters also vary as the power grid changes its operational regime (behavior of equipment in laboratory and in-filed conditions is quite different). Consequently, many different techniques have been developed in recent decades that provide an alternative way of determining the parameters of dynamic elements and power system stability, using real-time measurements for this purpose.

First steps in this direction were taken 30 years ago and they were applied on synchronous generators using the theory of trajectory sensitivity [2, 3]. These methods were significantly improved later in [4, 5]. In order to simplify the problem of parameter identification, values of some of them are specified in advance. Generally, this is usually done with parameters whose values do not significantly affect the accuracy of the dynamic model. Due to the correlation among parameters, the parameter estimation problem is usually over-parameterized, which leads to problems with numerical stability. In general, the parameter estimation depends on the number of unknown parameters and the available set of real-time measurements. In cases where there is a small number of measurements and many parameters that need to estimated, the optimization criterion (for example, the minimum least-squared error of measurement deviations) becomes insensitive to large parts of the parameter space, so multiple local solutions occur.

Parameter identification based on information geometry is proposed in [6]. This approach was verified on several types of dynamic elements in power system, such as synchronous generator, direct drive synchronous generator (DDSG), and doubly-fed induction generator (DFIG), which is examined in this paper. However, this method is highly sophisticated and for it to be used, very complex and numerically demanding mathematical simulations have to be performed.

This paper deals with the problem of nonlinear optimization of proportional-integral (PI) controller parameters in DFIG, which is modeled by a set of DAEs, connected to a power system, which is considered to be not known. The basic purposes of PI controllers are secondary regulation of the speed–active power and reactive power–voltage of multiple DFIGs connected in the same point (for example, a wind farm). The integral gain (term I in PI controller) is added, as it makes it possible to reach steady state condition without minimum state and algebraic variable deviations. In case of a major disturbance, power system stability and characteristics of transient response are determined by both proportional and integral gains. To calculate optimal parameters of the PI controllers, an 'Extremum Seeking' (ES) algorithm was used, more precisely, its version that assumes that gradient can be calculated [hence the name 'Gradient Extremum Seeking' (GES)]. The introduced assumption is that DFIG model and measurements are known in the connection point to the power system, which means that derivatives of the measurement with respect to PI controller parameters can be calculated (with uncertain and adjustable parameters).

The basic assumptions used in this paper are:

1. Model of the entire power system is *not known*,
2. DFIG model that is being examined and used to optimize parameters *is known*, and it is only employed when calculating the necessary gradients,
3. Measurements in the connection point to the power system *are known*.

These assumptions actually mean that the particular DFIG 'observes' all the variations of other grid elements and whole power system only through measurements in the connection point. These measurements are its only way of getting information about the rest of the power system behavior.

The main goal of this paper is to tune PI controller parameters, so that when a certain (typically major) disturbance(s) occurs, transient responses should be appropriate in a given sense. The criterion of optimality will be mean squared error over time and will be introduced in Section 3. The calculations are not meant to be done in real-time, but rather in advance, before DFIG (i.e. wind turbine or wind farm) is installed and connected to the power system. The input data used to adjust (optimize) PI parameters is taken from a history database, which stores all (or only typical) time responses for list of major disturbances that happened in the power system. The proposed algorithm makes use of this data (measurements) and gradients (obtained from DFIG model), to iteratively tune PI parameters, so that when a disturbance really happens, power system behaves in a desired way.

The paper is organized as follows. The DAEs that describe DFIG and measurement model which will be used in the tuning process (parameter optimization) will be introduced in Section 2. In Sections 3 and 4, a detailed mathematical description of the 'Extremum Seeking' algorithm and implementation details will be provided. Section 5 will present the results obtained by applying this algorithm to the IEEE 14-bus test system. Section 6 will give some conclusions and suggestions that could yield further improvement. Finally, used references are listed in Section 7, while details about DFIG modeling are given in Appendix (Section 8).

## 2 Models of Power System Elements and Measurements

Description of DFIG model is given in more details in Appendix. Here, only the compact form of equations will be written. Control loops used to pitch angle control, speed–active power control and reactive power–voltage control are also briefly explained in Appendix.

The DAEs model is the consequence of the existence of different time scales, and can be written in the following form [7]:

$$\frac{\mathrm{d}\boldsymbol{x}}{\mathrm{d}t} = \boldsymbol{f}\left(\boldsymbol{x}, \boldsymbol{z}, \boldsymbol{p}, t\right), \tag{1}$$

$$0 = \boldsymbol{g}\left(\boldsymbol{x}, \boldsymbol{z}, \boldsymbol{p}, t\right), \tag{2}$$

where:

$\boldsymbol{x}$ – vector of state variables;

$\boldsymbol{z}$ – vector of algebraic variables;

$\boldsymbol{p}$ – vector of parameters;

$\boldsymbol{t}$ – time (scalar variable).

The vector of measurements can be written in the following form:

$$y = \boldsymbol{h}\left(\boldsymbol{x}, \boldsymbol{z}, \boldsymbol{p}, t\right). \tag{3}$$

Variables that are contained in measurement vector ($\boldsymbol{y}$), i.e. that are being measured typically are active and reactive power which DFIG supplies to the power system ($P_g$ and $Q_g$ respectively) and complex voltage in the connection point [this complex voltage is represented by voltage magnitude ($V$) and angle ($\theta$)] – note that the voltage angle measurement is available from Phasor Measurement Unit (PMU) based measurements.

## 3 'Extremum Seeking' (ES) Basics

There are different approaches that deal with the problem of parameter tuning (optimization). Some of them require the full model of the power system

to be given. Although these methods usually work satisfactorily, it should be noted that this information is not available in most real-world cases. On the other hand, there are optimization approaches that start with the assumption that the power system model is not known (or it is partially known – gray-box approaches), but input/output measurements are [2 – 7], which is also a basic assumption in this paper. One such algorithm is called 'Extremum Seeking' (ES), which does not require the explicit knowledge of the input-output model, but only the existence of extremum in the optimization criterion, which corresponds to the desired behavior of the closed-loop system and the availability of input/output observations (measurements) [8, 9]. This is what makes ES so robust and widely used in industry practice (for an overview of practical applications, see [10]). Another benefit of this algorithm is that it can be applied both when nonlinearity is present in the process itself (in the form of physics-based nonlinearity), but also when the nonlinearity is present in the optimization criterion, which needs to be minimized.

The optimization criterion, that is the system's performance measure, can be represented as:

$$J(\boldsymbol{p}) = \wp(\boldsymbol{y}, \boldsymbol{p}), \tag{4}$$

where $\wp$ is the formal mathematical description of the system's response quality. The optimization criterion, $J(\boldsymbol{p})$ has one (global) or multiple (local) minimums, and our task is to find them, by applying ES. It is important to keep in mind that optimization criterion, $J(\boldsymbol{p})$ is not a measurement vector itself, but rather a measure of the desired power system's behavior. In this paper, the optimization criterion is defined as:

$$J(\boldsymbol{p}) \triangleq \sum_{d \in \mathfrak{D}} \frac{1}{T - t_0} \int_{t_0}^{T} \mathrm{e}^2(\boldsymbol{p}, d, t)\,\mathrm{d}t = \sum_{d \in \mathfrak{D}} \frac{1}{T - t_0} \int_{t_0}^{T} \left(\boldsymbol{y}(d,t) - \boldsymbol{y}_r\right)^2 \mathrm{d}t\,, \tag{5}$$

where $\boldsymbol{y} = \boldsymbol{h}(\boldsymbol{x}, \boldsymbol{z}, \boldsymbol{p}, t)$ is vector of measurements (3) and $\boldsymbol{y}_r$ represents a desired referent time response (constant, pre-disturbance value), while $\mathfrak{D}$ is the list of major disturbances for the optimization (recorded and stored in a historical database).

The goal of optimization is to find such set of optimal parameters ( $\boldsymbol{p}^*$ ) so that:

$$\boldsymbol{p}^* = \min_{\boldsymbol{p}} \left\{ J(\boldsymbol{p}) \right\}. \tag{6}$$

Since ES is basically a gradient method, one must not forget that parameters obtained in this procedure will not necessarily be a global minimum.

Nevertheless, this does not diminish the significance of the results, as in most cases a physically satisfactory solution is obtained.

The main feature of the algorithm is that it comes to an optimal solution gradually, by iteratively modifying the input (vector $\boldsymbol{p}$) of optimization criterion, $J(\boldsymbol{p})$, until an extremum is reached. Since the measurements in the connection point to the power system are assumed to be known, then the derivatives of the measurement functions, $\boldsymbol{y}=\boldsymbol{h}(\boldsymbol{x},\boldsymbol{z},\boldsymbol{p},t)$, with respect to PI controller parameters, $\partial\boldsymbol{y}/\partial\boldsymbol{p}$, are also known (with uncertain parameters). The vector $\boldsymbol{p}$ will be modified iteratively in the following manner:

$$\dot{\boldsymbol{p}}=\boldsymbol{K}\otimes\frac{\mathrm{d}J(\boldsymbol{p})}{\mathrm{d}\boldsymbol{p}}=\boldsymbol{K}\otimes\frac{\mathrm{d}\wp(\boldsymbol{y},\boldsymbol{p})}{\mathrm{d}\boldsymbol{p}}=\boldsymbol{K}\otimes\boldsymbol{f}\left(\frac{\mathrm{d}\boldsymbol{y}}{\mathrm{d}\boldsymbol{p}}\right),\quad \boldsymbol{K}>0, \tag{7}$$

where $\otimes$ is a symbol of Hadamard product.

If $\boldsymbol{p}^*$ is the value for which the measure of performance, $J(\boldsymbol{p})=\wp(\boldsymbol{y},\boldsymbol{p})$, reaches a minimum, then let us choose Lyapunov function candidate to be:

$$V=\wp\left(\boldsymbol{y},\boldsymbol{p}^*\right)-\wp\left(\boldsymbol{y},\boldsymbol{p}\right). \tag{8}$$

In this case, its derivative is:

$$\begin{aligned}\dot{V}&=\frac{\mathrm{d}\wp\left(\boldsymbol{y},\boldsymbol{p}^*\right)}{\mathrm{d}t}-\frac{\mathrm{d}\wp\left(\boldsymbol{y},\boldsymbol{p}\right)}{\mathrm{d}t}=0-\frac{\mathrm{d}\wp\left(\boldsymbol{y},\boldsymbol{p}\right)}{\mathrm{d}t}=\\&=-\frac{\mathrm{d}\wp\left(\boldsymbol{y},\boldsymbol{p}\right)}{\mathrm{d}\boldsymbol{p}}\frac{\mathrm{d}\boldsymbol{p}}{\mathrm{d}t}=-\frac{\mathrm{d}\wp\left(\boldsymbol{y},\boldsymbol{p}\right)}{\mathrm{d}\boldsymbol{p}}\dot{\boldsymbol{p}}.\end{aligned} \tag{9}$$

By combining (7) and (9), we have:

$$\dot{V}=-\frac{\mathrm{d}\wp\left(\boldsymbol{y},\boldsymbol{p}\right)}{\mathrm{d}\boldsymbol{p}}\otimes\boldsymbol{K}\otimes\frac{\mathrm{d}\wp\left(\boldsymbol{y},\boldsymbol{p}\right)}{\mathrm{d}\boldsymbol{p}}=-\boldsymbol{K}\otimes\left(\frac{\mathrm{d}\wp\left(\boldsymbol{y},\boldsymbol{p}\right)}{\mathrm{d}\boldsymbol{p}}\right)^2\le 0. \tag{10}$$

From the previous analysis, applying the Lyapunov method, it can be concluded that $\boldsymbol{p}$ converges to $\boldsymbol{p}^*$, which is an invariant set, meaning that equilibrium $\boldsymbol{p}^*$ is locally asymptotically stable. The same can be also proved if extremum is local maximum, simply by changing the signs of $\boldsymbol{K}$ and $V$.

If (7) and (5) are combined, we finally get optimization method for updating the parameters:

$$\dot{\boldsymbol{p}}=\boldsymbol{K}\otimes\int_{t_0}^{T}\left(\sum_{i=1}^{N_m}\frac{\partial\boldsymbol{y}_i(t)}{\partial\boldsymbol{p}}\otimes\left(\boldsymbol{y}_i(t)-\boldsymbol{y}_{ri}(t_0)\right)\right)\mathrm{d}t\,. \tag{11}$$

## 4 The Proposed Algorithm for Parameter Optimization

The optimization criterion, $J(\boldsymbol{p})$, can be understood as mapping from the parameters of the PI controller (vector $\boldsymbol{p}$) to the performance representation of the power system [$J(\boldsymbol{p})$ in (5)]. The 'Extremum Seeking' (ES) algorithm tunes the parameters, trying to minimize optimization criterion, $J(\boldsymbol{p})$. As mentioned above, because ES is essentially a gradient method, calculated parameters will not necessarily give a global optimum. The entire 'Gradient Extremum Seeking' (GES) algorithm for optimizing PI controller parameters is illustrated in Fig. 1. The experiment with transient analysis after mayor disturbance (for example, short circuit, branch outage etc.), which is shown within dashed lines, is performed iteratively. Optimization criterion, $J(\boldsymbol{p})$, is calculated at the end of transient analysis for list of major disturbances ($\mathfrak{D}$), where list $\mathfrak{D}$ contains different types of short circuits, load/generation outages and branch (line or transformer) single or multiple outages. GES algorithm then uses this value, $J(\boldsymbol{p}(k))$, to calculate new values of the PI controller parameters, $\boldsymbol{p}(k+1)$, where $k$ is the number of current iteration.

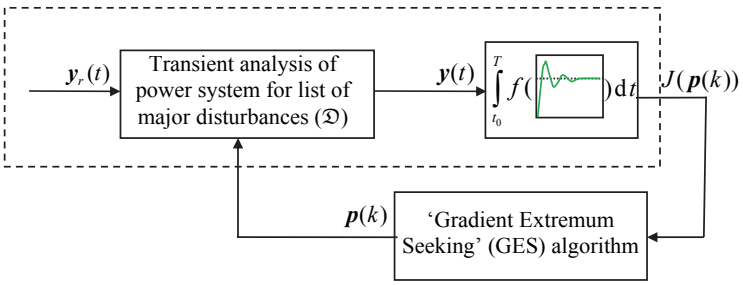


**Fig. 1 –** *Illustration of the GES algorithm for optimizing the PI controller parameters.*

Whereas Fig. 1 gives only a brief outline of the algorithm, flow-chart shown in Fig. 2 contains a more detailed explanation. Constant $\varepsilon$ represents the convergence criterion and determines when the algorithm stops (in this case, the value $\varepsilon = 10^{-9}$ was adopted). The initial value of the $\boldsymbol{K}$ vector was chosen to be $\boldsymbol{K} = [4 \cdot 10^{-8}; 4 \cdot 10^{-8}; 2 \cdot 10^{-6}; 2 \cdot 10^{-6}]^{\mathrm{T}}$. The process of assigning a value to $\boldsymbol{K}$ was empirical, but with intention that $\boldsymbol{K}$ achieves approximately the same increments for all parameters in the vector $\boldsymbol{p}$. In addition, the upper and lower limits of parameter values have been introduced, in order to ensure that during the iterations, parameters do not get unrealistically large or small values. Furthermore, it is assumed that, for the adopted range of parameters $\boldsymbol{0} \le \boldsymbol{p}^* \le \boldsymbol{p}^{\max}$, the optimization criterion does not have multiple extrema. Instead, it is presumed to be convex, which in this case is fulfilled.

Finally, in regard to the main motivation for this paper (optimization of PI controller parameters in DFIG only from local DAEs model of DFIG and available measurements in connection point to the power system), transient analysis needs more explanation. Equations (1) and (2) represent the general case. However, since in this paper we are only interested in DFIG, these equations get clearly defined form, given by (A3) and (A4). Due to their complexity, these equations had to be moved to Appendix, and only their shortened version is given here [(12) and (13)]. So, even though (1) and (2) resemble (12) and (13), it should be noted that they represent different concepts, or:

$$\frac{\mathrm{d}\boldsymbol{x}_{DFIG}}{\mathrm{d}t} = \boldsymbol{f}_{DFIG}\left(\boldsymbol{x}_{DFIG}, \boldsymbol{z}_{DFIG}, \boldsymbol{p}, t\right), \tag{12}$$

$$0 = \boldsymbol{g}_{DFIG}\left(\boldsymbol{x}_{DFIG}, \boldsymbol{z}_{DFIG}, \boldsymbol{p}, t\right), \tag{13}$$

where $\boldsymbol{f}_{DFIG}$ is given in (A3), $\boldsymbol{g}_{DFIG}$ is given in (A4), as well as $\boldsymbol{x}_{DFIG} = \left[\omega_m \quad \theta_p \quad x_1 \quad i_{rd} \quad x_2 \quad i_{rq}\right]^{\mathrm{T}}$ and $\boldsymbol{z}_{DFIG} = P_w^*\left(\omega_m\right)$, with additional algebraic equations for active and reactive bus power balances, respectively:

$$P_{DFIG} = P_{inj}, \tag{14a}$$

$$Q_{DFIG} = Q_{inj}. \tag{14b}$$

Transient analysis solves the DAEs model (12), (13), subject to the measurement constraints:

$$P_{DFIG} = P_m, \tag{15a}$$

$$Q_{DFIG} = Q_m, \tag{15b}$$

$$V = V_m, \tag{15c}$$

$$\theta = \theta_m, \tag{15d}$$

where measurement vector is represented as $\boldsymbol{y} = \left[P_m \quad Q_m \quad V_m \quad \theta_m\right]^{\mathrm{T}}$, where $P_m$, $Q_m$, $V_m$, and $\theta_m$ are measured active power, reactive power, voltage magnitude and voltage angle in bus where DFIG is connected to the power network, respectively.

## 5 Application and Discussion

In order to implement and test the proposed GES algorithm, Matlab environment was used, more precisely Power System Analysis Toolbox (PSAT) [11], where PSAT is used to generate measurements in the connection point (to

replace unavailable real-time measurements). In PSAT, the entire DAEs model of DFIG with PI controllers (as given in Appendix) was implemented. The original IEEE 14-bus test system has been modified, to include, in addition to synchronous generators (SG), also direct drive synchronous generators (DDSG, commonly used for modeling solar panels and wind turbines), and doubly-fed induction generators (DFIG, mostly used for modeling modern designs of wind generator and wind farm). In this paper, DFIG connected to the Bus 6 (the one within the red rectangle in Fig. 3) was analyzed. In Bus 6 are connected 30 identical wind units (which form a wind farm), with total installed apparent power $30\times2 = 60$ MVA. Note that the central controller for wind farm is applied, where the controller's output is shared in the same portion to the participating units.

Analyzed DFIG is described by:

– Six differential equations (A3), described by six state variables (vector $\boldsymbol{x}$): $\omega_m$, $\theta_p$, $x_1$, $i_{rd}$, $x_2$, and $i_{rq}$, where $\omega_m$ is rotor angular speed, $\theta_p$ is pitch angle, $i_{rd}$ and $i_{rq}$ are rotor currents in *d*- and *q*-axis, respectively, and $x_1$ and $x_2$ are two state variables introduced by integral gain of the controller (more details can be found in Appendix);

– One algebraic equation (A4), described by one algebraic variable (vector $\boldsymbol{z}$): $P_w^*(\omega_m)$;

– Two algebraic equations for active (A5) and reactive power balances (A6) in point (bus) where DFIG is connected, described by two algebraic variables of complex voltage in connection bus (vector $\boldsymbol{z}$): $V_6$ and $\theta_6$, and

– Four parameters: $k_{p1}$, $k_{i1}$, $k_{p2}$, and $k_{i2}$.

The aim of transient analysis is to determine whether the power system remains stable after major disturbance (such as short circuits, (dis)connection of large loads/generators etc.). The power system is considered to be stable if after a disturbance electromechanical oscillations are damped in time and if there are no large variations of variables. Usually, a period immediately after the disturbance is the most critical.

A schematic representation of the implementation of the transient analysis for single major disturbance from the list of major disturbances ($d \in \mathfrak{D}$) of a power system is given in Fig. 4.

The explanation of the transient analysis of the power system (for single major disturbance), shown in Fig. 4, can be summarized as follows. In the steady-state, the power-flow study is carried out in order to determine the operating condition of the power system.

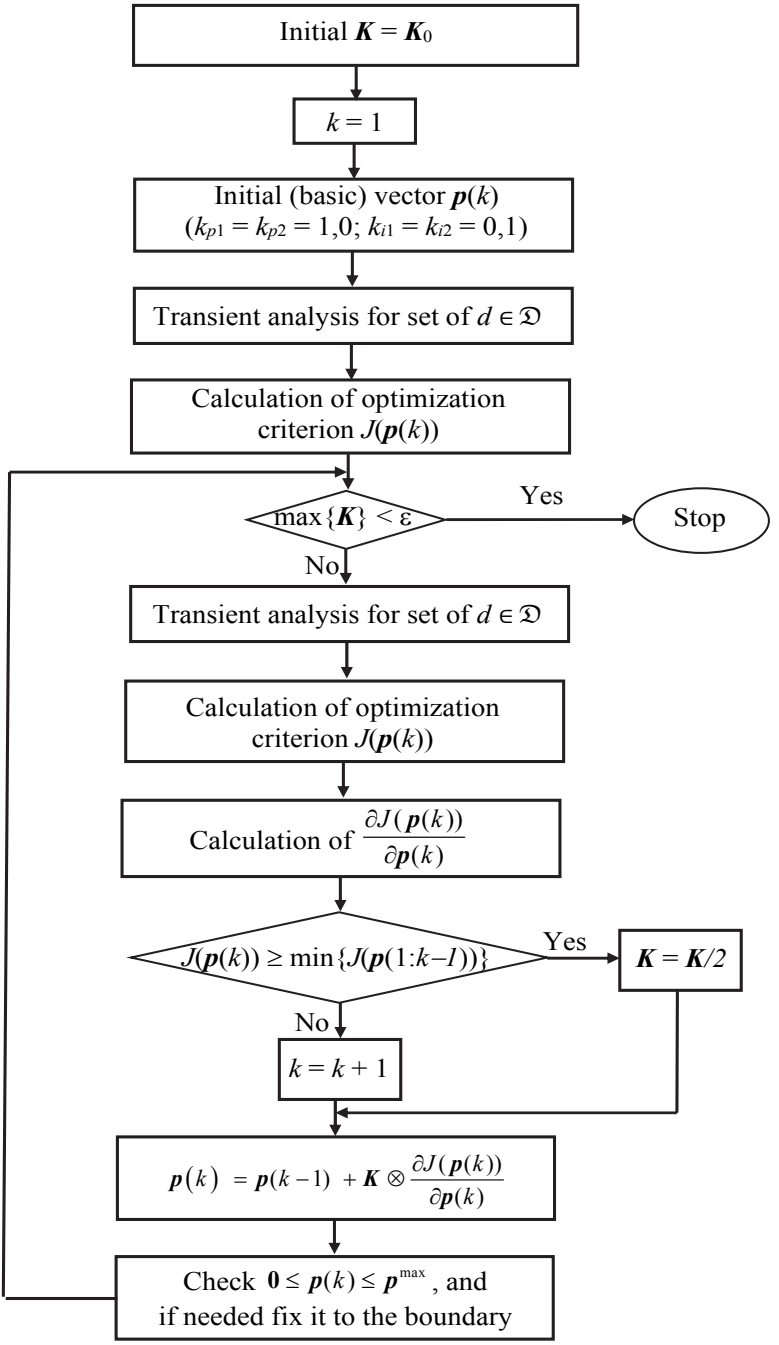


**Fig. 2 –** *Flow-chart of the proposed GES algorithm.*

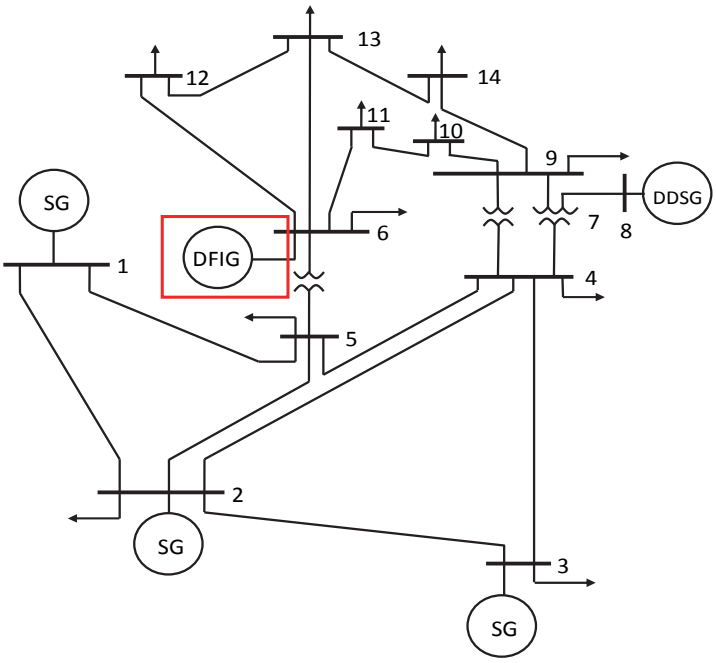


**Fig. 3 –** *Modified IEEE 14-bus test system with three types of distributed sources (SG, DDSG, and DFIG).*

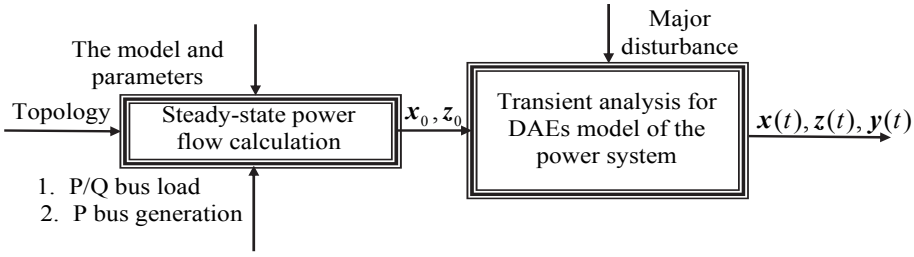


**Fig. 4 –** *Implementation of the transient analysis in the power system.*

The necessary input data are:

1. Topology of the power system;
2. Models of elements and their parameters (as a rule, catalog data is used);
3. Condition dependent inputs (active and reactive loads, as well as active power generations), which change in accordance with their daily profiles.

Details of this calculation will not be given here, as they are not so relevant to the problem analyzed in this paper. The result of the power-flow study is the

operating condition before major disturbance of the power system, described by vector of state variables ($\boldsymbol{x}_0$) and vector of algebraic variables ($\boldsymbol{z}_0$). In the steady-state, the power balance in the entire system is achieved, meaning that both active and reactive power productions are equal to active and reactive consumptions plus losses. If a major disturbance occurs anywhere in the power system, it will lead to the transient responses of state and algebraic variables. To calculate the transient responses, PSAT is used. This program will solve DAEs model (see Sections 2 and 4) and return transients of $\boldsymbol{x}(t), \boldsymbol{z}(t), \boldsymbol{y}(t)$. This information is then used to optimize PI controller parameters, so that with these parameters a power system behaves in a desired way.

Finally, a major disturbance that will lead to the unsatisfactory transients has to be specified. In this paper, for the given IEEE 14-bus test system, the transient will be caused by opening the switch on the branch 2-4 (see Fig. 3), and then closing it 200 ms later. For the initial values of the parameters (vector $\boldsymbol{p}$) are used ones from [7].

Sensitivity of measurements (vector function $\boldsymbol{h}$) with respect to PI controller parameters (vector $\boldsymbol{p}$), or $\partial \boldsymbol{h} / \partial \boldsymbol{p}$, are shown in Figs. 5a−d. Note that these sensitivities are calculated by:

$$\frac{\partial \boldsymbol{h}}{\partial \boldsymbol{p}} = \frac{\partial \boldsymbol{h}(\boldsymbol{x},\boldsymbol{z},\boldsymbol{p},t)}{\partial \boldsymbol{x}} \bullet \frac{\partial \boldsymbol{x}}{\partial \boldsymbol{p}} + \frac{\partial \boldsymbol{h}(\boldsymbol{x},\boldsymbol{z},\boldsymbol{p},t)}{\partial \boldsymbol{z}} \bullet \frac{\partial \boldsymbol{z}}{\partial \boldsymbol{p}} + \frac{\partial \boldsymbol{h}(\boldsymbol{x},\boldsymbol{z},\boldsymbol{p},t)}{\partial \boldsymbol{p}}, \tag{16}$$

where derivatives $\frac{\partial \boldsymbol{x}}{\partial \boldsymbol{p}}$ and $\frac{\partial \boldsymbol{z}}{\partial \boldsymbol{p}}$ are calculated from (1) and (2) respectively as:

$$\frac{d}{dt}\frac{\partial \boldsymbol{x}}{\partial \boldsymbol{p}} = \frac{\partial \boldsymbol{f}(\boldsymbol{x},\boldsymbol{z},\boldsymbol{p},t)}{\partial \boldsymbol{x}} \bullet \frac{\partial \boldsymbol{x}}{\partial \boldsymbol{p}} + \frac{\partial \boldsymbol{f}(\boldsymbol{x},\boldsymbol{z},\boldsymbol{p},t)}{\partial \boldsymbol{z}} \bullet \frac{\partial \boldsymbol{z}}{\partial \boldsymbol{p}} + \frac{\partial \boldsymbol{f}(\boldsymbol{x},\boldsymbol{z},\boldsymbol{p},t)}{\partial \boldsymbol{p}}, \tag{17}$$

$$0 = \frac{\partial \boldsymbol{g}(\boldsymbol{x},\boldsymbol{z},\boldsymbol{p},t)}{\partial \boldsymbol{x}} \bullet \frac{\partial \boldsymbol{x}}{\partial \boldsymbol{p}} + \frac{\partial \boldsymbol{g}(\boldsymbol{x},\boldsymbol{z},\boldsymbol{p},t)}{\partial \boldsymbol{z}} \bullet \frac{\partial \boldsymbol{z}}{\partial \boldsymbol{p}} + \frac{\partial \boldsymbol{g}(\boldsymbol{x},\boldsymbol{z},\boldsymbol{p},t)}{\partial \boldsymbol{p}}. \tag{18}$$

Also, note that ‘Basic’ sensitivities in Figs. 5a–d denote time variation of measurements, $\boldsymbol{h}(\boldsymbol{x},\boldsymbol{z},\boldsymbol{p},t)$, without additional derivatives introduced in (16). Also, note that in these plots there are the same sensitivities (the same figure shapes).

Let us analyze the influence of vector $\boldsymbol{p}$ to the vector function $\boldsymbol{h}$ (composed with active and reactive powers and bus voltage magnitude and angle). By performing numerous simulations, one concludes that some parameters have a considerable effect on the transient responses, while the influence of others is negligible. Let us look at, for example, how the reactive power ($Q_g$) changes when the parameter $k_{p1}$ is varied. It is easy to conclude that the time variation

of response drastically changes, and even stability can be critical. On the other hand, the influence of parameter $k_{i1}$ on the voltage angle ( $\theta$ ) is small, as can be seen from Fig. 6.

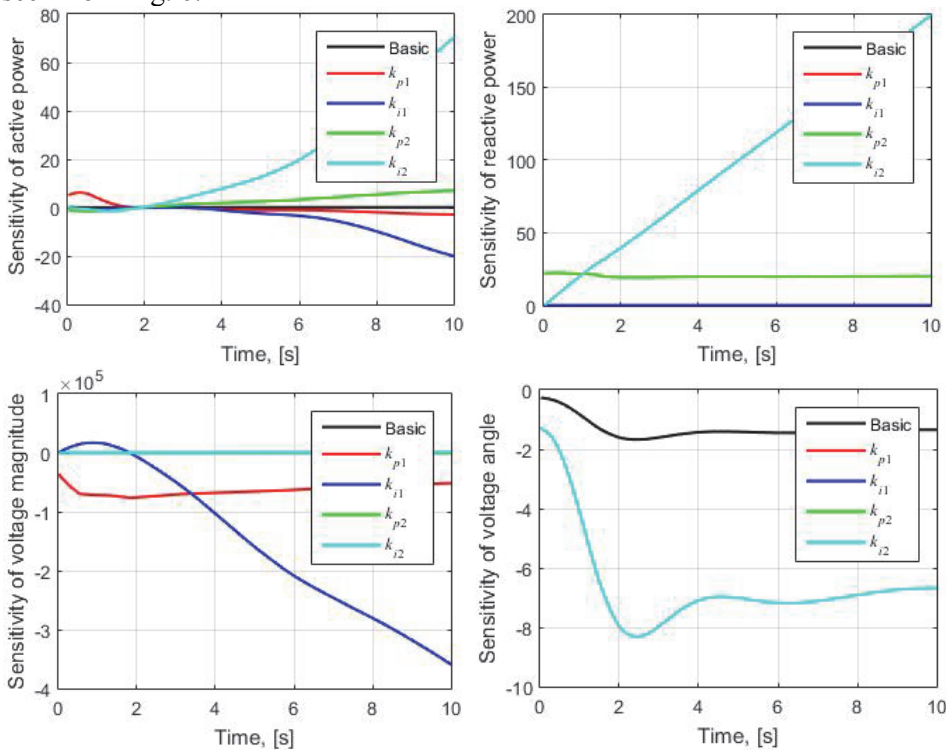


**Fig. 5 –** *Sensitivity of measurements (vector function* ***h****) with respect to PI controller parameters (vector* ***p****).*

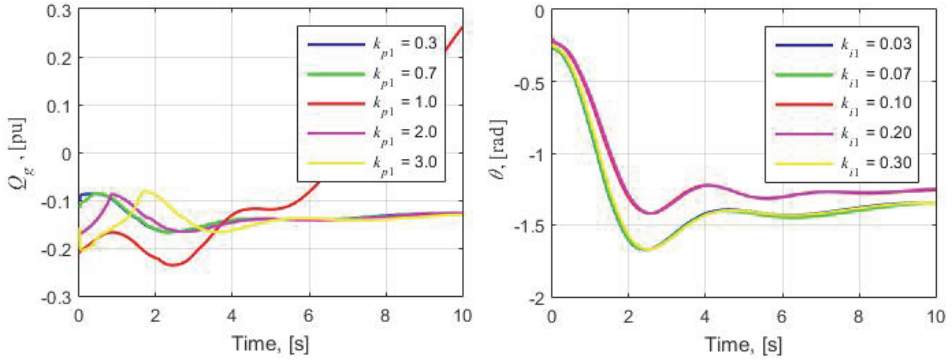


(a) *The influence of* $\boldsymbol{k}_{p1}$ *on reactive power* ($\boldsymbol{Q}_g$). (b) *The influence of* $\boldsymbol{k}_{i1}$ *on voltage angle* $\boldsymbol{\theta}$.

**Fig. 6 –** *The influence of PI controller parameters to the measured variables.*

Taking into account all conclusions made above, the optimization was carried out using the GES algorithm. The results obtained for each iteration of the algorithm are shown in **Table 1**.

**Table 1**
*Step-by-step results of the GES algorithm.*

| Number of iteration | Optimization criterion ($J$) | $K$ for $k_{p1}$ | $K$ for $k_{i1}$ | $K$ for $k_{p2}$ | $K$ for $k_{i2}$ | $k_{p1}$ | $k_{I1}$ | $k_{p2}$ | $k_{i2}$ |
|---|---|---|---|---|---|---|---|---|---|
| 1 | 576.39 | $4.0{\cdot}10^{-8}$ | $4.0{\cdot}10^{-8}$ | $2.0{\cdot}10^{-6}$ | $2.0{\cdot}10^{-6}$ | 1.000 | 0.100 | 1.000 | 0.100 |
| 2 | 562.20 | $4.0{\cdot}10^{-8}$ | $4.0{\cdot}10^{-8}$ | $2.0{\cdot}10^{-6}$ | $2.0{\cdot}10^{-6}$ | 1.102 | 0.350 | 1.002 | 0.061 |
| 3 | 562.07 | $1.0{\cdot}10^{-8}$ | $1.0{\cdot}10^{-8}$ | $5.0{\cdot}10^{-7}$ | $5.0{\cdot}10^{-7}$ | 1.127 | 0.415 | 1.002 | 0.050 |
| 4 | 548.38 | $2.5{\cdot}10^{-9}$ | $2.5{\cdot}10^{-9}$ | $1.25{\cdot}10^{-7}$ | $1.25{\cdot}10^{-7}$ | 1.134 | 0.432 | 1.002 | 0.047 |
| 5 | 544.25 | $3.9{\cdot}10^{-11}$ | $3.9{\cdot}10^{-11}$ | $1.95{\cdot}10^{-9}$ | $1.95{\cdot}10^{-9}$ | 1.135 | 0.435 | 1.002 | 0.046 |

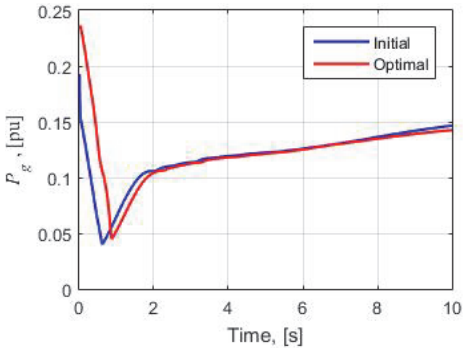


(a) *Active power*

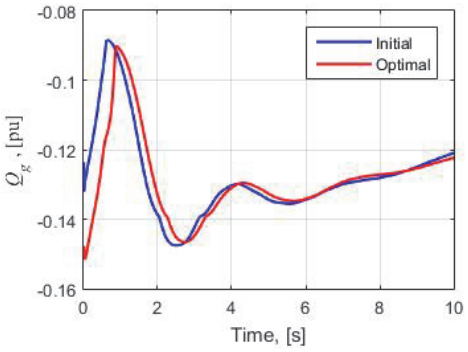


(b) *Reactive power*

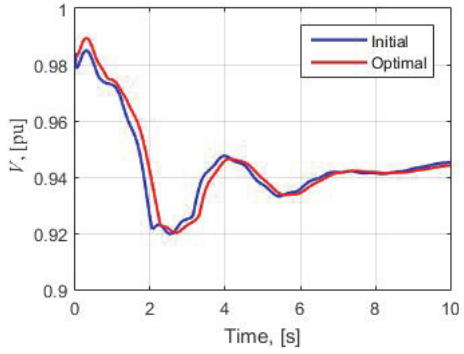


(c) *Voltage magnitude in connection bus*

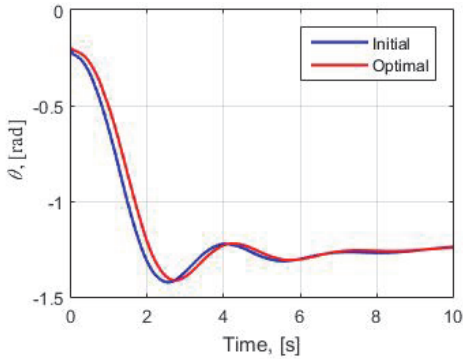


(d) *Voltage angle in connection bus*

**Fig. 7 –** *Transient responses of available measurements in the connection bus for initial (basic) and optimal PI controller parameters of DFIG.*

Fig. 7 shows the responses of the active and reactive powers, as well as voltage magnitude and angle, before (initial, basic) and after parameter optimization using the GES method. By analyzing the obtained results, it can be concluded that the total decrease in the value of the optimization criterion is around 5.6 %, which can prove to be significant, especially in large-scale power systems. The importance of this result is even greater when one considers that improper values of PI controller parameters may even threaten stability, as was the case in Fig. 6a.

Due to high nonlinearity of the analyzed problem, the optimal solution depends on the initial parameter values. As mentioned before, the optimization criterion [ $J(\boldsymbol{p})$ ] can be understood as mapping from the parameters of the PI controllers (vector $\boldsymbol{p}$) to the performance representation of the power system. In other words, we are moving through the 4-dimensional space trying to find a point where $J$ will be as little as possible. In case there are multiple minimums, the point in this space from which the optimization begins will determine in which minimum we will end. Some of them are local minimums, and only one is global. Simply stated, this means that the problem has multiple suboptimal solutions. This is particularly true for integral gains of PI controllers, whose variations do not affect value of $J$ so much. Starting from a different point will often lead to different results and when tuning parameters there is almost always room for progress.

## 6 Conclusion

In this paper, the problem of optimization of proportional-integral (PI) controller parameters in doubly-fed induction generator (DFIG) is analyzed. DFIG is commonly used for connections to both distribution and transmission networks. It is an integral part of the wind farms, which are getting more popular as demand for clean and renewable energy grows. To optimize the PI controller parameters, the modified Gradient Extremum Seeking algorithm was proposed, where the least squared error was chosen in the optimization criterion. The obtained results show that applied nonlinear optimization produced favorable results by decreasing the optimization criterion by approximately 5.6 %.

The obtained results suggest the way for further development of the algorithm and future research on this topic. For example, additional analysis could be done, to see how the optimal solution would change if different optimization criterion is introduced. In addition, weights on certain measurements can be introduced, by increasing/decreasing effect they have on the optimization criterion. For instance, one could alter the criterion so that the active/reactive power have a dominant effect on optimization criterion, while voltage magnitude and angle would affect it less. Another modification that

seems to be promising is to change the optimization starting point and increment steps. As was already mentioned, Extremum Seeking is a gradient method, so changing the point from which the optimization starts could result in different (and possibly) better set of optimal parameters. Finally, more robust methods for time-dependent nonlinear optimization can be investigated.

## 7 Acknowledgement

The authors would like to thank the Ministry of Education, Science and Technological Development of the Republic of Serbia for the support of this work within the project No. TR32038.

## 8 Appendix

### 8.1 DFIG Model

DFIG consists of an induction generator with a round rotor. Its stator is directly connected to the three-phase power grid (with the small frequency variation around rated value, 50 Hz), while rotor in equipped with a bidirectional 'back-to-back' voltage converter. The term 'doubly-fed' refers to the fact that stator is directly connected to the power grid, whereas the rotor's voltage is generated using a voltage converter (Fig. A1). Such DFIG's construction enable the operation in a wide range of speeds. The converter compensates the difference between mechanical and electrical torque, by injecting rotor current of variable frequency. This means that voltage converter and controllers, both during the normal and contingency conditions, determine the behavior of the electrical machine.

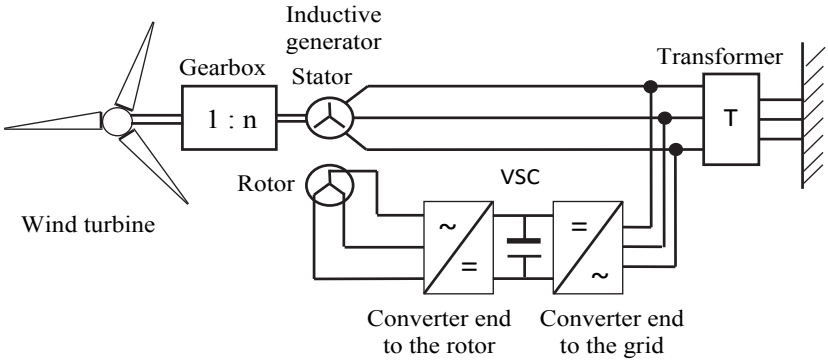


**Fig. A1 –** *Model of the DFIG [12, 13].*

DFIG consists of the following components, shown in Fig. A1 [12, 13]:

– wind turbine;

– gearbox;
– inductive generator;
– Voltage Sourced Converter (VSC), which connects the rotor and the power grid and consists of two converters connected by a DC link;
– speed–active power regulation;
– reactive power–voltage regulation;
– pitch angle (torque) regulation.

Wind turbine provides the constant mechanical torque ( $\tau_m = P_w / \omega_m$ , where $P_w$ is wind power and $\omega_m$ is rotor angular speed). It is assumed that the effect of gearbox is negligible.

## 8.2 Control loops

Control loops used to control pitch angle, speed–active power and reactive power–voltage are shown in Figs. A2−A4, respectively [7, 14, 15].

*Control of pitch angle:* Taking into account that the wind turbine is under the influence of a stochastic wind variation, it is necessary to control the mechanical power that is transferred to the wind turbine. This is done by altering the pitch angle of wind turbine blades (Fig. A2). For this reason, a negative feedback loop is created, in which angular speed of turbine ( $\omega_t$ ) is compared to the setpoint value ( $\omega_{ref}$ ), resulting in an error signal which is an input to the controller. The output is the pitch angle change ( $\theta_p$ ), leading to the mechanical power change, $P_w^*(\omega_m)$.

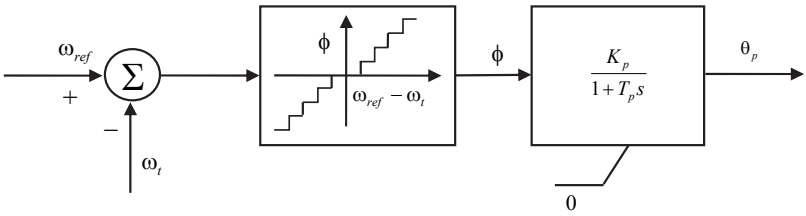


**Fig. A2 –** *Control loop for pitch angle regulation.*

*Control of speed–active power:* The aim of this control loop, in which the first PI regulator is located, is to maintain the frequency closest to the rated value (50 Hz). When this is the case, the system's active power balance is achieved, meaning that the production of all generators is equal to consumption plus the losses. The active power control is achieved by regulating the DFIG's angular speed. When there is a deficit of active power, a decrease in the DFIG's

speed leads to the frequency drop. Opposite condition happens when there is more active power than needed. For this control loop, input variables are: mechanical power of the wind turbine [$P_w^*(\omega_m)$], turbine angular speed ($\omega_m$), and active power that DFIG supplies to the power grid ($P_g$), see Fig. A3. Due to the presence of PI controller, additional differential equation is introduced:

$$\frac{\mathrm{d}x_1}{\mathrm{d}t} = \tau_t^* - \tau_e = \frac{P_w^*}{\omega_m} - \frac{P_g}{\omega_m}. \tag{A1}$$

with a new state variable for first PI controller, called $x_1$.

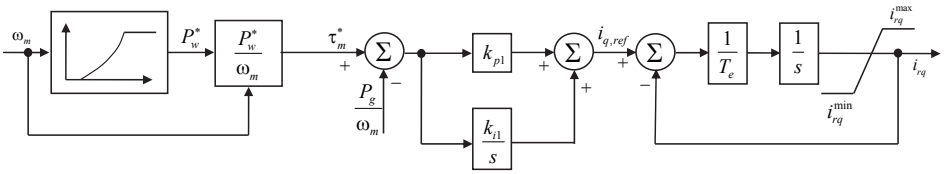


**Fig. A3 –** *Control loop for speed–active power regulation.*

*Control of reactive power–voltage:* The task of this control loop is to maintain the required reactive power of the DFIG (note that the bus voltage in connection point is maintained by the reactive power), which is done using VSC. Reactive power of DFIG ($Q_g$) is compared to the desired value ($Q_{g,ref}$). If there is a difference between these two values, an input signal is generated for the additional differential equation, introduced by the second PI controller:

$$\frac{\mathrm{d}x_2}{\mathrm{d}t} = Q_{g,ref} - Q_g, \tag{A2}$$

with a new state variable for second PI controller, called $x_2$.

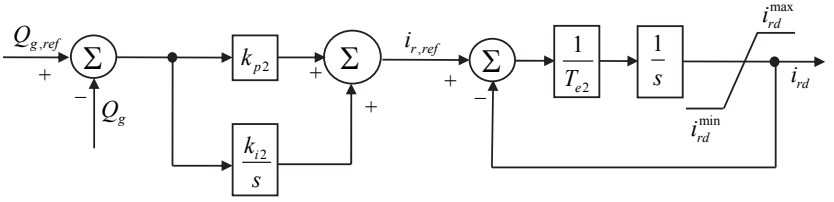


**Fig. A4 –** *Control loop for reactive power–voltage regulation.*

### 8.3 Differential-Algebraic Equations (DAEs) of DFIG model

DFIG shown in Fig. A1 can be described by the following DAEs, respectively [7, 11 – 15]:

$$f \Rightarrow \begin{cases} \dfrac{\mathrm{d}\omega_m}{\mathrm{d}t} = \dfrac{\tau_t - \tau_e}{2H_m} = \dfrac{P_w/\omega_m - P_g/\omega_m}{2H_m}, \\ \dfrac{\mathrm{d}\theta_p}{\mathrm{d}t} = \dfrac{1}{T_p}\left[K_p\phi\left(\omega_{ref} - \omega_m\right) - \theta_p\right], \\ \dfrac{\mathrm{d}x_1}{\mathrm{d}t} = \tau_t^* - \tau_e = \dfrac{P_w^*}{\omega_m} - \dfrac{P_g}{\omega_m}, \\ \dfrac{\mathrm{d}i_{rq}}{\mathrm{d}t} = \dfrac{1}{T_e}\left[k_{p1}\left(\dfrac{P_w^*}{\omega_m} - \dfrac{P_g}{\omega_m}\right) + k_{i1}x_1 - i_{rq}\right], \\ \dfrac{\mathrm{d}x_2}{\mathrm{d}t} = Q_{g,ref} - Q_g, \\ \dfrac{\mathrm{d}i_{rd}}{\mathrm{d}t} = \dfrac{1}{T_{e2}}\left(i_{r,ref} - i_{rd}\right) = \dfrac{1}{T_{e2}}\left[k_{p2}\left(Q_{g,ref} - Q_g\right) + k_{i2}x_2 - i_{rd}\right], \end{cases} \tag{A3}$$

$$g \Rightarrow P_w^*\left(\omega_m\right) = \begin{cases} 0, & \text{if} \quad \omega_m < 0,5, \\ 2\omega_m - 1, & \text{if} \quad 0,5 \le \omega_m \le 1, \\ 1, & \text{if} \quad \omega_m > 1, \end{cases} \tag{A4}$$

where:

$$\tau_t = P_w/\omega_t = \tau_m = P_w/\omega_m \,,$$

$$\tau_e = x_\mu\left(i_{rq}i_{sd} - i_{rd}i_{sq}\right) = \frac{P_g}{\omega_m} \approx -\frac{x_\mu V i_{rq}}{\omega_m\left(x_s + x_\mu\right)},$$

$$P_g = v_{sd}i_{sd} + v_{sq}i_{sq} + v_{rd}i_{rd} + v_{rq}i_{rq} \approx Vi_{sq} = -\frac{x_\mu V}{x_s + x_\mu}i_{rq},$$

$$Q_g = v_{sq}i_{sd} - v_{sd}i_{sq} + v_{rq}i_{rd} - v_{rd}i_{rq} \approx Vi_{sd} = -\frac{x_\mu V i_{rd}}{x_s + x_\mu} - \frac{V^2}{x_s + x_\mu},$$

$$i_{sq} = -\frac{x_\mu}{x_s + x_\mu}i_{rq}\,,\; i_{sd} = -\frac{x_\mu i_{rd}}{x_s + x_\mu} - \frac{V}{x_s + x_\mu}\,.$$

### 8.4 Algebraic Equations (AEs) of point (bus) where DFIG is connected

These equations represent bus active and reactive power balances (assumed that no loads connected to this bus), respectively:

$$P_g = P_{inj} = \sum_{j=1}^{N} V_i V_j \left(G_{ij}\cos(\theta_i - \theta_j) + B_{ij}\sin(\theta_i - \theta_j)\right), \tag{A5}$$

$$Q_g = Q_{inj} = \sum_{j=1}^{N} V_i V_j \left(G_{ij}\sin(\theta_i - \theta_j) - B_{ij}\cos(\theta_i - \theta_j)\right), \tag{A6}$$

where $P_{inj}$ and $Q_{inj}$ are active and reactive power injections to the power network, respectively, while $N$ is number of buses in the power system.

## 9 References


[1] G. Andersson, P. Donalek, R. Farmer, N. Hatziargyriou, I. Kamwa, P. Kundur, et al.: Causes of the 2003 Major Grid Blackouts in North America and Europe, and Recommended Means to Improve System Dynamic Performance, IEEE Transactions on Power Systems, Vol. 20, No. 4, November 2005, pp. 1922 – 1928.

[2] J. J. Sanchez-Gasca, C. J. Bridenbaugh, C. E. J. Bowler, J. S. Edmonds: Trajectory Sensitivity Based Identification of Synchronous Generator and Excitation System Parameters, IEEE Transactions on Power Systems, Vol. 3, No. 4, November 1988, pp. 1814 – 1822.

[3] S. M. Benchluch, J. H. Chow: A Trajectory Sensitivity Method for the Identification of Nonlinear Excitation System Models, IEEE Transactions on Energy Conversion, Vol. 8, No. 2, June 1993, pp. 159 – 164.

[4] I. A. Hiskens: Nonlinear Dynamic Model Evaluation from Disturbance Measurements, IEEE Transactions on Power Systems, Vol. 16, No. 4, November 2001, pp. 702 – 710.

[5] M. Burth, G. C. Verghese, M. Velez-Reyes: Subset Selection for Improved Parameter Estimation in On-Line Identification of a Synchronous Generator, IEEE Transactions on Power Systems, Vol. 14, No. 1, February 1999, pp. 218 – 225.

[6] M. K. Transtrum, A. T. Sarić, A. M. Stanković: Information Geometry Approach to Verification of Dynamic Models in Power Systems, IEEE Transactions on Power Systems, Vol. 33, No. 1, January 2018, pp. 440 – 450.

[7] A. T. Sarić, M. K. Transtrum, A. M. Stanković: Information Geometry for Model Identification and Parameter Estimation in Renewable Energy – DFIG Plant Case, IET Generation, Transmission & Distribution, Vol. 12, No. 6, March 2018, pp. 1294 – 1302.

[8] K. B. Ariyur, M. Krstić: Real-Time Optimization by Extremum-Seeking Control, John Wiley & Sons, Inc., Hoboken, New Jersey, USA, 2003.

[9] N. J. Killingsworth, M. Krstic: PID Tuning Using Extremum Seeking: Online, Model-Free Performance Optimization, IEEE Control Systems Magazine, Vol. 26, No. 1, February 2006, pp. 70 – 79.

[10] A. Lj. Marjanović: Thermal Power Plant Boiler Temperature Distribution Control Based on Extremum Seeking Strategy, Doctoral Dissertation, School of Electrical Engineering, University of Belgrade, 2017. (in Serbian)

[11] F. Milano: Power System Modelling and Scripting, Springer, London, UK, 2010.

[12] J. Machowski, J. W. Bialek, J. R. Bumby: Power Systems Dynamics: Stability and Control, 2nd Edition, Jon Wiley & Sons Ltd., Hoboken, New Jersey, USA, 2008.

[13] Wind Power in Power Systems, Edited by T. Ackermann, Jon Wiley & Sons Ltd., Chichester, England, 2005.

[14] H. A. Pulgar-Painemal, P. W. Sauer: Reduced-Order Model of Type-C Wind Turbine Generators, Electric Power Systems Research, Vol. 81, No. 4, April 2011, pp. 840 – 845.

[15] Wind turbines – Part 27-1: Electrical Simulation Models-Wind Turbines, IEC Std 61400-27-1:2015, 2015.